Materials Transactions, Vol. 48, No. 9 (2007) pp. 2464 to 2466

Preparation of TiO_2 Nanotubes and Their Photocatalytic Properties in Degradation Methylcyclohexane

Wen Liu, Jianqin Gao, Fengbao Zhang* and Guoliang Zhang

School of Chemical Engineering & Technology, Tianjin University, Tianjin 300072, P. R. China

The tubular TiO_2 photocatalysts were successfully synthesized by hydrothermal method. The external tube diameters fall in 8 and 12 nm and the internal diameters are between 5 and 8 nm. Moreover, the lengths of the nanotubes are up to 500 nm and the specific surface area increases to 330 m^2/g, while TiO_2 powders are 78 m^2/g. Methylcyclohexane (MCH) was selected as the target pollutant to investigate the photocatalytic performance. The results indicate that TiO_2 nanotubes accelerate the degradation of MCH under the same conditions, comparing with TiO_2 nanoparticles. Finally, the degradation reaction shows a first order kinetics. [doi:10.2320/matertrans.MRA2007616]

(Received March 22, 2007; Accepted July 2, 2007; Published August 22, 2007)

Keywords: *titanium oxide, nanotubes, photocatalysis, methylcyclohexane, kinetics*

1. Introduction

Many environmental problems are expected to be solved with the aid of photocatalysts. Titanium oxide (TiO_2) features excellent photocatalytic properties[1–3] because of their wide band gap. It can be used in degradation of many pollutants, including liquid and gas phases. Now, a great deal of effort is under progress to enhance the photocatalytic performance by widening the wavelength sensitization range with the additives of various ions, such as nitrogen, Fe^{3+}, V^+, Ag, Sn^{2+} and Al^{3+}.[4–9] However, little work focus on changing the morphology of the photocatalysts to degrade the pollutant effectively. Moreover, it has been reported that TiO_2 showed superior when specific surface area increases.[10] Therefore, TiO_2 nanotubes have been found to give some advantages over TiO_2 nanoparticles because of their larger specific surface area.[11]

TiO_2 nanotubes can be prepared by the template[12,13] and hydrothermal technology.[14,15] Comparing with hydrothermal method, TiO_2 nanotubes prepared by template have larger tube diameters, thicker tube wall and smaller specific surface area. In this paper, TiO_2 nanotubes were synthesized from TiO_2 crystals by hydrothermal process and their photocatalytic activity and kinetics to methylcyclohexane (MCH) were studied.

2. Experimental

2.1 Synthesis of TiO_2 nanotubes photocatalyst by hydrothermal method

All chemicals were of analytical grade and used without further purification. The method employed for the synthesis of TiO_2 nanotubes was similar to described in Ref. 16), except where otherwise indicated. In the experimental synthesis, 4.0 g pure TiO_2 powders, a mixture of anatase and rutile type coexisted, was mixed with 60 ml 10 $kmol/m^3$ NaOH aqueous solution in a Teflon-lined autoclave at 120°C for 20 h. The powders after the alkali-treatment were rinsed well with distilled water, and further rinsed with 0.1 $kmol/m^3$ HCl solution followed by distilled water until the pH reached around 7. The obtained white sample was dried at 80°C for 5 h. The specific surface area of the sample before chemical treatment was 78 m^2/g. However, it increased markedly to 330 m^2/g after chemical treatment.

*Corresponding author, E-mail: fbzhang@tju.edu.cn

2.2 Characterization of the TiO_2 nanotubes photocatalyst

The prepared TiO_2 nanotubes photocatalysts were characterized by X-ray diffraction (XRD, Rigaku D/max 2500v/pc, Japan) using a Cu Kα source ($\lambda = 0.154056$ nm), and transmission electron microscopy (TEM, JEM-100 CX II, Japan). The Brunauer–Emmett–Teller (BET, NOVA-2000, USA) surface area (S_{BET}) of the samples was obtained from nitrogen adsorption–desorption data.

2.3 Photocatalytic activity measurements

The photocatalytic properties of TiO_2 nanotubes photocatalyst were evaluated by photo-degradation of gas MCH. The photocatalytic reaction was performed under ultraviolet irradiation by using a 10 W ultraviolet lamp. The initial concentration of MCH was 100 mg/m^3 in a batch reactor with a volume of 26 L at room temperature (25°C). The 1.0 g photocatalysts were covered on a 0.013 m^2 glass plank. The MCH gas was stirred for 30 min without ultraviolet irradiation to allow the system to reach an adsorption-desorption equilibrium. Then the analytical samples were drawn from the reactor every 15 min during the whole reaction. The concentrations of MCH were analyzed by gas chromatogram (GC, 6890N, Agilent Technologies).

3. Results and Discussion

3.1 XRD analysis

Figure 1 shows the XRD patterns of TiO_2 nanotubes calcined at 450°C for 2 h (a), TiO_2 nanoparticles (b) and untreated TiO_2 nanotubes (c), respectively. It can be seen the anatase coexisted with rutile phases in the starting material, while after chemical treatment, the TiO_2 nanoparticles were transformed into tubular morphology and the width of the diffraction peaks became large with the strength becoming weak. The inset in Fig. 2(d) shows the disorder lattice layer of the sidewalls, implying the poor crystallinity of the TiO_2

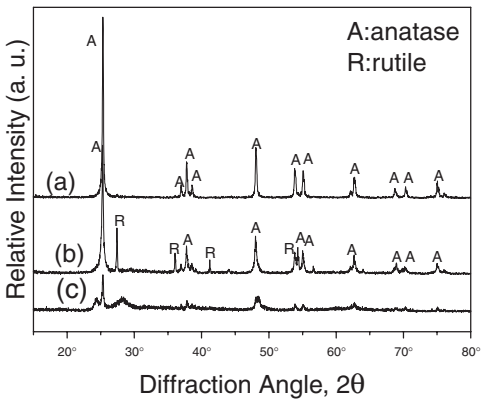

Fig. 1 XRD patterns of TiO_2 nanotubes calcined at 450°C for 2 h (a), TiO_2 nanoparticles (b) and untreated TiO_2 nanotubes (c).

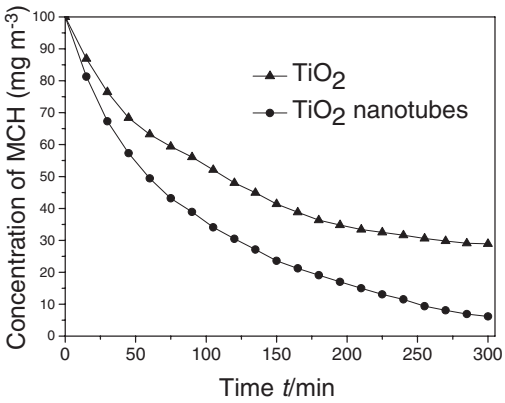

Fig. 3 Effect of TiO_2 photocatalysts on removal efficiency of MCH.

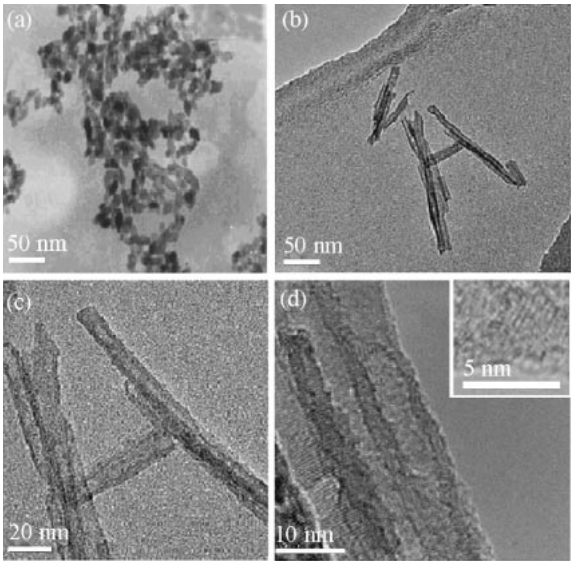

Fig. 2 TEM images of the TiO_2 nanoparticles (a) and prepared titanate nanotubes atdifferent times (b, c and d). The scale bars in (a), (b), (c), (d) and its inset are 50, 50, 20, 10 and 5 nm, respectively.

nanotubes. After calcination at 450°C for 2 h, the TiO_2 nanotubes transformed to anatase, which was in good agreement with other studies.[17–19)]

3.2 Morphology of titanate nanotubes

Figure 2 shows the TEM images of the starting material and the prepared TiO_2 nanotubes. It can be seen the starting material exhibits nanoparticles type and the mean diameters are about 20 nm. After hydrothermal synthesis, the particles were completely converted to TiO_2 nanotubes. Furthermore, the external tube diameters fall in 8–12 nm and the internal diameters are between 5 and 8 nm. The lengths of nanotubes are up to 500 nm. Comparing with the TiO_2 nanotubes reported previously, the TiO_2 nanotubes in this study have smaller tube diameters and thinner tube wall.[20,21)] Due to the transmission of electron under TEM (Fig. 2), the edges of a TiO_2 nanotube along the axis show deeper gray color compared with that in the center, implying the tubular structure similar to that of a carbon nanotube.[22)] It can be also observed that the end of a TiO_2 nanotube is open without a closed tip (different from some common carbon nanotube).

3.3 Photo-catalytic activity

The photocatalytic activities of the titania nanotubes films were evaluated by the degradation test of MCH. Titania films with the same surface areas and the same thickness prepared by sol-gel method[21)] were also studied under identical conditions to compare their photocatalytic effects with the titania nanotubes. The results are given in Fig. 3. As shown, the gas MCH has been more effectively degraded by the films of titania nanotubes. After 300 min, the degradation ratio of gas MCH on titania nanotubes films was 95%, whereas it was 72% on titania films. The TiO_2 nanotubes have large specific surface area (330 m^2/g tested by BET) and hollow tubular structures (as shown in Fig. 2), attributing to a higher quantum yield compared with common TiO_2 nanoparticles. However, it was observed that the rate decreased during irradiation, suggesting a deactivation of the catalyst.

3.4 The reaction kinetics of gas MCH

Under our experimental conditions, the reaction order and rate constant of the degradation of gas MCH on TiO_2 nanotubes were investigated. Figure 4 shows that the relationship between ln (C_A/C_0) and time is of good linearity, so the degradation of MCH exhibits first order kinetics, matching well with the classic Langmuir-Hinshelwood (LH) model. In the LH model, the reaction of degradation follows a rate determining step where an adsorbed molecule reacts with a reactive transient such as a OH^g radical formed on the surface by oxidation of H_2O or a surface OH^- group. The reaction rate should be proportional to the surface coverage by MCH molecules.

According to the simple Langmuir model for the MCH adsorption, the reaction rate is given by the relationship: $r = k_{deg}K_{LH}C/(1 + K_{LH}C)$, where K_{LH} is the adsorption constant, C, the MCH concentration in the gas phase and k_{deg}, a kinetic constant. The constant K_{LH} relates to an effective gas toluene adsorption rather than the actual adsorption on the catalyst. A discrepancy between the actual adsorption constant and that of the L-H model has already been pointed out.[23)] The constant k_{deg} (mol min^{-1} m^{-2}) is associated with the reactive system and depends on experimental conditions such as the initial concentration, the catalyst thickness, the absorbed light flux and the temperature.

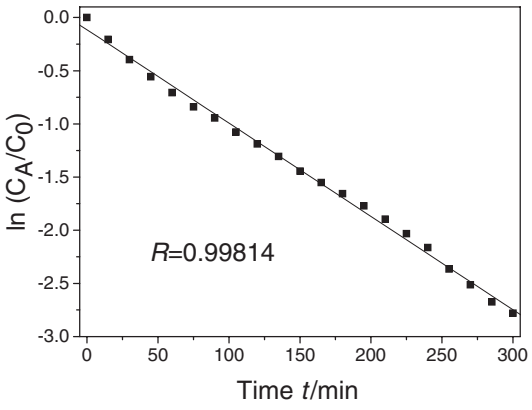

Fig. 4 The relationship between ln (C_A/C_0) and time.

4. Conclusions

TiO_2 nanotubes have been prepared with the hydrothermal method. They are expected to have a high performance as the photocatalysts. By using MCH as target pollutant, we have tested the photocatalytic performance. The results display the TiO_2 nanotubes have better photocatalytic activity than the TiO_2 nanoparticles. Under our experimental conditions, MCH was decreased by 95% on TiO_2 nanotubes, while it was 72% on TiO_2 particles. Furthermore, the degradation of MCH exhibits the first order kinetics, which in agreement with the simple L-H model.

REFERENCES

1) A. Fujishima and K. Honda: Nature **238** (1972) 37–38.
2) H. Yamashita, Y. Ichihashi and M. Anpo: Hyomen Kagaku **16** (1995) 194–199.
3) T. Kasuga, M. Hiramatu, M. Hirano, A. Hoson and K. Oyamada: J. Mater. Res. **12** (1997) 607–613.
4) B. Wawrzyniak and A. W. Morawski: App. Cata. B: Envir. **62** (2006) 150–158.
5) J. G. Yu, H. G. Yu, C. H. Ao, S. C. Lee, J. C. Yu and W. K. Ho: Thin Solid Films **496** (2006) 273–280.
6) X. G. Hou, F. H. Hao, B. Fan, X. N. Gu, X. Y. Wu and A. D. Liu: Nucl. Instrum. Meth. B **243** (2006) 99–102.
7) S. Rengaraj and X. Z. Li: J. Mol. Cata. A: Chem. **243** (2006) 60–67.
8) H. C. Lee and W. S. Hwang: Mater. Trans. **46** (2005) 1942–1949.
9) D. F. Wang and J. H. Ye: Mater. Trans. **46** (2005) 2699–2703.
10) C. H. Kwon, H. Shin, J. H. Kim, W. S. Choi and K. H. Yoon: Mater. Chem. Phys. **86** (2004) 78–82.
11) J. C. Xu, M. Lu, X. Y. Guo and H. L. Li: J. Mol. Cata. A: Chem. **226** (2005) 123–127.
12) R. W. Kerr: *Chemistry and Industry of Starch* (Academic Press, New York, 1950) pp. 325–328.
13) S. Ikeno, T. Kawabata, H. Hayashi, K. Matsuda, S. Rengakuji, T. Suzuki, Y. Hatano and K. Tanaka: Mater. Trans. **43** (2002) 939–945.
14) T. Lindstrom and C. Soermark: Thin Solid Films & Interface Sci. **55** (1976) 305–312.
15) S. D. Hammid and D. C. Sherrington: Polym. **28** (1987) 325–331.
16) T. Kasuga: Thin Solid Films **496** (2006) 141–145.
17) X. M. Sun and Y. D. Li: Chem. Eur. J. **9** (2003) 2229–2238.
18) R. Ma, Y. Bando and T. Sasaki: Chem. Phys. Lett. **380** (2003) 577–582.
19) C. C. Tsai and H. Teng: Chem. Mater. **16** (2004) 4352–4358.
20) Y. Lan, X. Gao, H. Zhu, Z. Zheng, T. Yan, F. Wu, S. P. Ringer and D. Song: Adv. Funct. Mater. **15** (2005) 1310–1318.
21) C. Ren, B. Zhong, H. Liu and Y. Zhang: J. Chem. Eng. Chin. Univ. **18** (2004) 57–61.
22) S. Lijima: Nature **354** (1991) 56–58.
23) N. Doucet, F. Bocquillon, O. Zahraa and M. Bouchy: Chemosphere **65** (2006) 1188–1196.